Wavelength tuning and switching of a coupled distributed feedback and Fabry–Perot cavity laser

M. C. Wu, M. M. Boenke, M. Werner, F. Schiffmann, Y. H. Lo, and S. Wang

Citation: Journal of Applied Physics **63**, 291 (1988); doi: 10.1063/1.340292
View online: http://dx.doi.org/10.1063/1.340292
View Table of Contents: http://scitation.aip.org/content/aip/journal/jap/63/2?ver=pdfcov
Published by the AIP Publishing

Wavelength tuning and switching of a coupled distributed feedback and Fabry–Perot cavity laser

M. C. Wu, M. M. Boenke, M. Werner, F. Schiffmann, Y. H. Lo, and S. Wang
Department of Electrical Engineering and Computer Sciences, Electronics Research Laboratory and Lawrence Berkeley Laboratory, University of California, Berkeley, California 94720

(Received 6 July 1987; accepted for publication 15 September 1987)

We present a theoretical analysis of a newly demonstrated semiconductor laser with coupled distributed feedback and Fabry–Perot (DFB-FP) cavities and show that three modes of operation are possible for such a laser. In mode-switched DFB mode, the wavelength can be switched between longitudinal modes on either side of the stopband. In coupled-cavity laser mode, there are successive mode hops inside the stopband. Finally, in continuously tunable distributed Bragg reflector mode, a wide wavelength tuning range (4.8 Å) without mode hopping can be obtained. The analysis is general enough to be applied to any laser with a periodic waveguide section, and provides an understanding of the mechanisms and the limits of wavelength tuning in such lasers. This type of laser has very important applications in coherent optical communications.

INTRODUCTION

Stable single-frequency light sources are very important for optical communication systems. Distributed feedback (DFB)[1,2] and distributed Bragg reflector (DBR)[3] laser diodes are the most promising sources due to their single-longitudinal mode operation. Recently, there has been growing interest in coherent optical communications, such as frequency modulation[4] and frequency shift keying,[4] because of the higher information transmission rates possible. For these applications wavelength tuning and switching are particularly important in addition to frequency stability.

Both tuning and switching of the wavelength have been demonstrated by coupled-cavity lasers.[5,6] However, the wavelengths of these lasers are very sensitive to the pumping currents and the coupling structures and are, therefore, not stable. Complicated optical and electrical feedback circuits are usually necessary to control the wavelength and prevent mode hopping. On the other hand, DFB lasers have demonstrated very stable single-frequency operation even under high-speed modulation[2] and large continuous wavelength tuning ranges are obtainable.[3] Therefore, the combination of a DFB section coupled with a Fabry–Perot (FP) section results in a laser which operates in a stable single frequency as a DFB laser, but can be continuously tuned and discretely switched in wavelength.

Recently such a laser has been built[7] and the mode-switching property was observed experimentally. With an additional phase control section, Murata, Mito, and Kobayashi[8] demonstrated a wide wavelength tuning range of 58 Å. However, up to now there is no theoretical analysis of such structures. To know the upper limit of the wavelength tuning range, a detailed understanding of the tuning mechanism is important. It is the purpose of this paper to present a systematic study of the wavelength tuning and switching behavior of such a coupled DFB-FP laser.

THEORETICAL FORMULATION

A schematic diagram of the coupled DFB-FP laser is shown in Fig. 1. It consists of a DFB section of length l_{DFB} and a FP section of length l_{FP}. The sections are separately pumped with the bias currents I_{DFB} and I_{FP}, respectively, to adjust the carrier densities and therefore the optical path lengths. Reflection occurs at the interface of the DFB and FP sections because the propagation constant of the DFB section is modified by the periodic pertubation of the refractive index. The coupling can be described by a scattering matrix S.[9] The propagation of optical waves in the DFB section is described by the forward propagation factor[9]

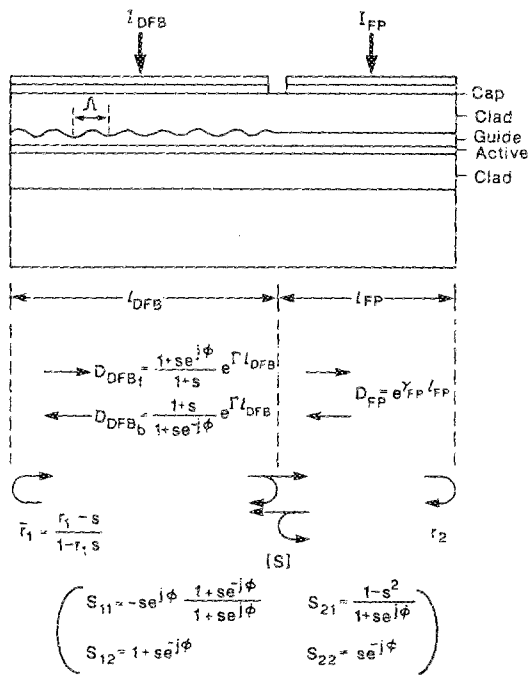

FIG. 1. The schematics of the coupled DFB-FP laser. The length of the DFB section is l_{DFB} and that of the FP section is l_{FP}. D_{DFB_f} and D_{DFB_b} are the propagation factors of a DFB laser in the forward and backward direction, respectively. The propagation factor in the FP section is D_{FP}. The S matrix characterizes the coupling between the DFB and FP sections. The r_1 and r_2 are the facet reflectivities and $\bar{r}_1$ is the effective reflectivity on the DFB side.

 0021-8979/88/020291-04$02.40

$$D_{\mathrm{DFB}_f} = e^{\Gamma l_{\mathrm{DFB}}}(1 + se^{j\phi})/(1 + s)$$

and the backward propagation factor

$$D_{\mathrm{DFB}_b} = e^{\Gamma l_{\mathrm{DFB}}}(1 + s)/(1 + se^{-j\phi}),$$

where $\phi = 2k_B l_{\mathrm{DFB}}$, $k_B = \pi/\Lambda$ is the Bragg wave vector, and Λ is the period of the index grating. The effective DFB reflection coefficient

$$s = j\kappa/[P + (g_{\mathrm{DFB}} + j\delta)],$$

where κ is the coupling coefficient of the grating, $\delta = \kappa_B - \beta_{\mathrm{DFB}}$ is the detuning from the Bragg wave vector, and $P^2 = (g_{\mathrm{DFB}} + j\delta)^2 + \kappa^2$. Also, $\Gamma = G - jK = P + jk_B$ is the effective propagation constant in the DFB section. Noting that $D_{\mathrm{FP}} = e^{(g_{\mathrm{FP}} - j\beta_{\mathrm{FP}})l_{\mathrm{FP}}}$ is the propagation factor in the FP section, the threshold equation can be obtained from the round trip condition,

$$1 - r_{\mathrm{eff}}^2 D_{\mathrm{DFB}_f} D_{\mathrm{DFB}_b} D_{\mathrm{FP}}^2 = 0. \quad (1)$$

Here, r_{eff} is given by[10]

$$r_{\mathrm{eff}}^2 = \bar{r}_1 r_2 (S_{12}S_{21} - S_{11}S_{22}) + S_{11}\bar{r}_1 (1/D_{\mathrm{FP}}^2) + S_{22} r_2 (1/D_{\mathrm{DFB}_f} D_{\mathrm{DFB}_b}), \quad (2)$$

where the S_{ij} are the elements of the scattering matrix,[9] $\bar{r}_1 = (r_1 - s)/(1 - r_1 s)$ is the reflectivity at the DFB end facet, and $r_2 = 0.56$ is just the reflectivity of the cleaved facet.

RESULTS AND DISCUSSION

The threshold condition Eq. (1) is analyzed numerically to find the threshold gain and lasing wavelength of a GaAs/AlGaAs laser. We assume linear gain and linear refractive index variation with injected current, which is good for threshold analysis. The extension of this analysis to above threshold will be discussed later. Figure 2 shows the threshold gain $g_{\mathrm{DFB}_{\mathrm{th}}} l_{\mathrm{DFB}}$ versus the detuning from the Bragg wave vector δl_{DFB} of the DFB section for $I_{\mathrm{FP}} = 0$ and $r_1 = 0.56$. The grating phase at the left facet is fixed at 0 and at the interface, it is determined by $\kappa_B l_{\mathrm{DFB}}$ ($\approx 0.6\pi$ in this case). The grating strength measured by κl_{DFB} increases from 0 to 1.5 for $l_{\mathrm{DFB}} = 100\ \mu$m and $l_{\mathrm{FP}} = 150\ \mu$m. Each curve represents one mode with κl_{DFB} as a parameter. When $\kappa l_{\mathrm{DFB}} = 0$, the DFB becomes a FP section and the reflection at the DFB-FP interface disappears because S reduces to the unit matrix. Therefore, it is exactly a FP laser of length $L = l_{\mathrm{DFB}} + l_{\mathrm{FP}}$. For finite values of κl_{DFB}, there are appreciable reflections at the DFB-FP interface due to non-zero S_{11} and S_{22}. Just as in a coupled-cavity laser, the threshold gain is modified by the interference effect between the DFB and FP cavities. For very large values of κl_{DFB}, the modes are very similar to that of a conventional DFB laser. The number of such DFB modes is less than the number of modes at $\kappa l_{\mathrm{DFB}} = 0$ (combined FP modes). This is reasonable because the DFB mode spacing ($\approx \pi/l_{\mathrm{DFB}}$) is larger than the combined FP mode spacing of $\pi/(l_{\mathrm{DFB}} + l_{\mathrm{FP}})$.

As the FP current I_{FP} increases, there are two effects. First, the additional gain in the FP section will reduce $I_{\mathrm{DFB}_{\mathrm{th}}}$. Second, the phase interference between DFB and FP can be modified so that discrete wavelength switching or continuous tuning is possible. Figure 3 shows the lowest threshold mode wavelength versus I_{FP} for $\kappa = 80\ \mathrm{cm}^{-1}$, $l_{\mathrm{DFB}} = 100\ \mu$m, and $l_{\mathrm{FP}} = 150\ \mu$m. The reflectivities at both facets are assumed to be 0.56. The active layer thickness is $0.2\ \mu$m and the width of the active region is $5\ \mu$m. The carrier lifetime is kept constant at 2 ns. The coupled DFB-FP laser operates in three different modes depending on the pumping currents I_{DFB} and I_{FP}. When $I_{\mathrm{FP}} < 8.8$ mA, the FP section is lossy and the laser operates in mode I, as a mode-switched DFB. The wavelength can be switched between the two DFB modes on either side of the stopband. Mode II occurs for I_{FP} between 8.8 and 12.5 mA, when there is gain in both sections and the laser operates in coupled-cavity mode. Successive mode hopping across the stopband is usually observed. Mode III is the continuously tunable DBR mode and occurs when the DFB section is lossy ($I_{\mathrm{FP}} > 12.5$ mA). In this case, the wavelength can be tuned continuously by the DFB current I_{DFB}.

In mode I, an increase in I_{FP} will shift the modes towards the negative δ side of the stopband. The in-phase mode may become out of phase and vice versa due to the phase change in the FP section, and the lowest $g_{\mathrm{DFB}_{\mathrm{th}}}$ mode may change. For example, at $I_{\mathrm{FP}} = 1.6$ mA, the wavelength switches from above stopband to below stopband (mode b to mode $\bar{c}$ in Fig. 2). At $I_{\mathrm{FP}} = 4.1$ mA, it switches back to above stopband (mode c). This phenomneon has been observed experimentally by Kitamura *et al.*,[7] however, their

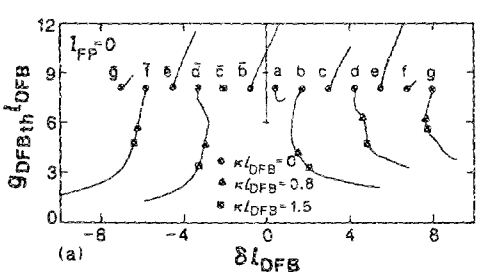

FIG. 2. The $g_{\mathrm{DFB}_{\mathrm{th}}} l_{\mathrm{DFB}}$ vs δl_{DFB} of the DFB-FP laser with $l_{\mathrm{DFB}} = 100\ \mu$m and $l_{\mathrm{FP}} = 150\ \mu$m for $I_{\mathrm{FP}} = 0$. Each curve represents a mode with κl_{DFB} as a parameter. The ● represents $\kappa = 0$, ▲ represents $\kappa = 80\ \mathrm{cm}^{-1}$, and ■ represents $\kappa = 150\ \mathrm{cm}^{-1}$.

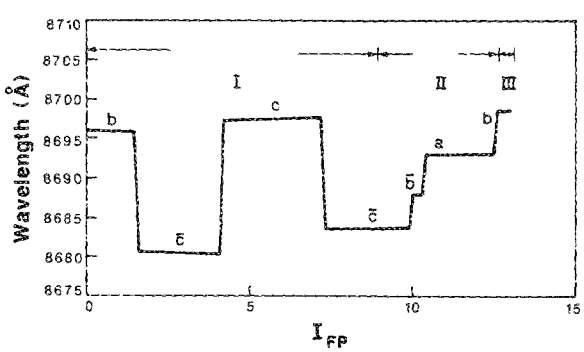

FIG. 3. The wavelength of the lowest $g_{\mathrm{DFB}_{\mathrm{th}}}$ mode vs the FP current I_{FP} for $\kappa = 80\ \mathrm{cm}^{-1}$, $l_{\mathrm{DFB}} = 100\ \mu$m and $l_{\mathrm{FP}} = 150\ \mu$m. The letters represent the different modes in Fig. 2. The range of I_{FP} is divided into three regions of different modes: region I is mode-switched DFB mode, region II is coupled-cavity laser mode, and region III is continuously tunable DBR mode.

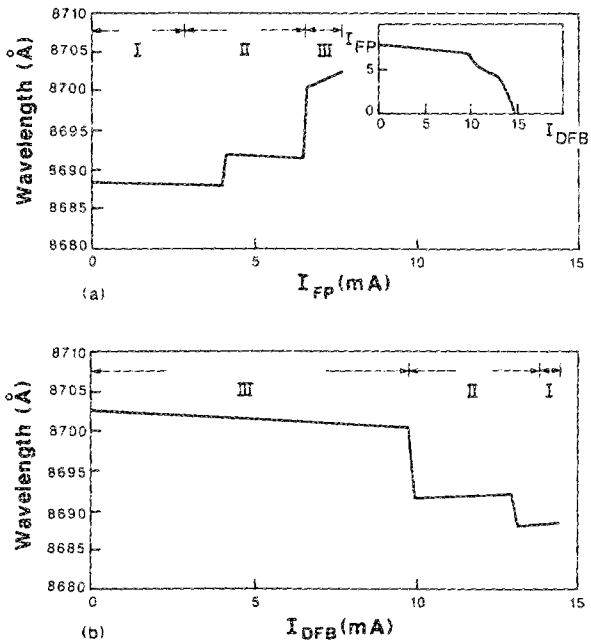

FIG. 4. (a) The wavelength of the lowest $g_{DFB_{th}}$ mode vs FP the current I_{FP}. (b) The same wavelength vs the DFB current I_{DFB} for $\kappa = 80\ cm^{-1}$, $l_{FP} = 200\,\mu m$ and $l_{DFB} = 50\,\mu m$. The three different regions of I_{DFB} or I_{FP} are the same as that of Fig. 3. This large ratio of l_{DFB}/l_{FP} is favorable for a large continuous tuning range. The inset of (a) shows the corresponding threshold I_{FP} for a given I_{DFB}. The I_{FP} is relatively insensitive to I_{DFB} for I_{DFB} less than 10 mA.

explanation based on variable-phase reflectivity is incomplete. They neglected the fact that there are more combined FP cavity modes than DFB modes and, therefore, the phase change needed for mode switching was overestimated. For example, when the wavelength returns to above the stopband at $I_{FP} = 4.1$ mA, it goes to mode *c* instead of mode *d* in Fig. 2.

When I_{FP} is larger than 8.8 mA, the current at which the FP section experiences no loss or gain, the coupled DFB-FP laser becomes more like a coupled-cavity laser. The successive mode hopping in Fig. 3 at $I_{FP} = 9.9$, 10.3, and 12.5 mA is very typical of coupled-cavity lasers. The difference is that the lasing mode is not determined by the gain profile of the laser, but instead by the narrow reflection band of the DFB section. Therefore, the hopping always occurs inside the stopband.

When I_{FP} is larger than 12.5 mA, the DFB section is lossy and the laser operates in mode III. The wavelength stops hopping and stays in the same mode. It can be tuned by changing the Bragg wavelength with I_{DFB} as in a DBR laser. This is the continuously-tunable DBR mode. The tuning range is larger for a large ratio of l_{DFB}/l_{FP} Figure 4(a) shows a similar plot of λ versus I_{FP} for $l_{DFB} = 200\,\mu m$ and $l_{FP} = 50\,\mu m$. For $I_{FP} > 6.5$ mA, there is a continuous tuning range of 1.9 Å. The inset shows the corresponding threshold I_{FP} for a given I_{DFB}. The I_{FP} is insensitive to variations of I_{DFB}, though the Bragg wavelength is very effectively shifted by I_{DFB}. The λ is plotted again with respect to I_{DFB} in Fig. 4 (b) to show more clearly the tuning range.

We also studied the effect of the grating ending position and the reflectivity at the DFB facet. Since the overall phase in a round trip can be modulated by I_{FP}, different grating ending position just corresponds to a shift in I_{FP}. This is confirmed by numerical simulation. When the DFB facet is antireflection coated, the $\Delta g_{DFB_{th}}$ between the two lowest $g_{DFB_{th}}$ modes is larger. Also the number of modes inside the stopbands decreases due to shorter effective length of the DFB section. Therefore, larger ΔI_{FP} is needed to switch wavelength back and forth on two sides of the stopband in mode I. The continuous tuning range in mode III is also increased because large I_{DFB} can be applied before mode hopping occurs. Simulation results show that for $l_{DFB} = 200\,\mu m$, $l_{FP} = 50\,\mu m$, the tuning range is 1.9 Å for $r_1 = 0.56$ and 2.2 Å for $r_1 = 0$. For longer l_{DFB} ($= 225\,\mu m$, $l_{FP} = 25\,\mu m$), 4.8 Å is achievable with $r_1 = 0$.

The 58-Å wavelength tuning range of the newly developed three-section DBR laser[8] can also be explained by our theory. The laser operates in mode II (coupled-cavity mode) and the additional phase control section is to bring one mode continuously to another inside the stopband instead of hopping. As was shown earlier, the maximum tuning range of $\Delta\delta$ is obtained when the mode moves across the stopband, $\Delta\delta_{max} \approx -a\kappa$, where $a \gtrsim 2$, depending on the coupling strength. Since $\Delta\delta = -\Delta\beta = 2\pi n\Delta\lambda/\lambda^2 - 2\pi\Delta n/\lambda$, the maximum wavelength tuned is

$$\Delta\lambda \approx \lambda(\Delta n/n) - (a\lambda^2/2\pi n)\kappa. \tag{3}$$

For a quaternary laser at $\lambda = 1.5\,\mu m$, $\kappa = 100\ cm^{-1}$, and $a \approx 3, \Delta\lambda \approx -60$ Å (minus means λ decreases with I_{DFB}), which agrees with the experimental results.

For practical purposes the laser has to operate above threshold, where the assumption of linear index variation with current is not valid. However, in modes I and III, either the DFB or the FP section is lossy and the carrier concentration is not clamped. The current can still be used to modulate the refractive index and optical path length effectively. Therefore, the threshold analysis here can still be applied in the more general case. Similar approximations of the nonlinear relations of gain and refractive index versus current as in Ref. 11 can be used.

CONCLUSION

In conclusion, we have presented an analysis based on simulation of the threshold condition which has general applicability to lasers with periodic waveguides. The results show that three modes of operation are possible for the coupled DFB-FP laser. Mode I occurs when the FP current I_{FP} is small and allows the wavelength to be switched between modes on either side of the stopband. This is useful for frequency-shift-keyed communciation systems because it provides externally controlled switching with the frequency stability of a DFB laser. When there is gain in both the DFB and FP sections, the laser operates in mode II, the coupled-cavity laser mode, and successive mode hopping across the stopband can be expected. With an additional phase control region, very wide tuning range across the stopband is possible. Mode III is the continuously tunable DBR mode, which occurs when the DFB section is lossy. A continuous tuning range (4.8 Å) is obtainable for a laser with a large ratio of l_{DFB}/l_{FP} and an antireflection coated DFB facet. The tuning

range can be further extended in a three-section laser. This type of operation is desirable for coherent communication systems because it allows continuous tuning under external modulation while providing the narrow linewidth of a DFB laser.

ACKNOWLEDGMENTS

This work was supported by National Science Foundation Grant No. ECS-8410838, Bell Northern Research, and Eastman Kodak.

[1]K. Kojima, S. Noda, S. Tai, K. Kyuma, K. Hamanaki, and T. Nakayama, Appl. Phys. Lett. **49**, 366 (1986).
[2]T. L. Koch, T. J. Bridges, E. G. Burkhardt, P. J. Corvini, L. A. Coldren, R. A. Linke, W. T. Tsang, R. A. Logan, L. F. Johnson, R. F. Kazarinov, R. Yen, and D. P. Wilt, Appl. Phys. Lett. **47**, 12 (1985).
[3]Y. Tohmori, H. Oohashi, T. Kato, S. Arai, K. Komori, and Y. Suematsu, in Proceedings of the Conference on Lasers and Electro-Optics (CLEO), San Francisco, 1986 (Optical Society of America, Washington, DC, 1986), paper No. WP3, p. 222.
[4]L. L. Jeromin and D. Welford, IEEE J. Lightwave Technol. **LT-4**,591 (1986).
[5]W. T. Tsang, N. A. Olsson, and R. A. Logan, Appl. Phys. Lett. **42**, 650 (1983).
[6]S. W. Corzine, L. A. Coldren, C. A Burrus, and T. L. Koch, Appl. Phys. Lett. **48**, 1190 (1986).
[7]M. Kitamura, M. Yamaguchi, K. Emura, I. Mito, and K. Kobayashi, IEEE J. Quantum Electron. **QE-21**, 415 (1985).
[8]S. Murata, I. Mito, and K. Kobayashi, *Technical Digest of Optical Fiber Communication Conference* (OFC), Reno, 1987 (Optical Society of America, Washington, DC, 1987), paper No. WC3.
[9]S. Wang, IEEE J. Quantum Electron. **QE-10**, 413 (1974).
[10]H.-K. Choi, K.-L. Chen, and S. Wang, IEEE J. Quantum Electron. **QE-20**, 385 (1984).
[11]L. A. Coldren and T. L. Koch, IEEE J. Quantum Electron. **QE-20**, 659 (1984).